The 21st Conference of Mechanical Engineering Network of Thailand
17-19 October 2007, Chonburi, Thailand

Local Void Fraction Measurement by using Reflected Ultrasonic Intensity and Wire Mesh Tomography in Air-Water Bubbly Flow

Nattadate Fuangworawong

Department of Mechanical Engineering, Faculty of Engineering,
Chulalongkorn University, Bangkok 10330, Thailand
Tel: 0-2218-6628, Fax: 0-2252-2889, E-mail: nattadate78@yahoo.com

Abstract

The objective of this work is to investigate characteristics of reflected ultrasonic signal in many bubbly flow conditions. Local void fraction of the flow conditions are clarified by using Wire Mesh Tomography (WMT). The experimental apparatus is a circular acrylic pipe with an inner diameter of 50 mm. This study applies ultrasonic signal and measures strength of reflected intensity from bubbles. The averaged and standard deviation of reflected ultrasonic intensity along an ultrasonic beam are obtained and reported. Local void fraction at same position with an ultrasonic probe by Wire Mesh Tomography (WMT) is also obtained and reported. In this work, it can be concluded that the averaged of reflected ultrasonic intensity, the standard deviation of reflected ultrasonic intensity and the local void fraction in the same flow condition have the same profile. These three parameters will be employed for database in development of local void fraction measurement by using reflected ultrasonic intensity in the future work.

Keywords: Local void fraction, Reflected ultrasonic intensity, Wire Mesh Tomography, Symmetric bubbly flow, Air-water system

1. Introduction

Bubbly flow behaviors play an important role for many industries, such as chemical industry, petrochemical industry, environmental industry, nuclear power industry and so on. Many measurement techniques, both intrusive and non-intrusive techniques, have been developed to investigate characteristics of bubbly flow. An ultrasonic technique is one of the non-intrusive measurement techniques proposed and developed by many researcher for decades. Ultrasonic measurement offers many advantages, such as cheaper, more simple, more safety than other measurement methods such as X-ray method, Gamma-ray method and so on. Furthermore, the ultrasonic method is a non-invasive measuring system. This method is also suitable for optically opaque systems and potentially applicable to high temperature and pressure conditions. Bubble velocity, liquid velocity and void fraction are important parameters in characteristic study of two-phase flow. The bubble velocity and liquid velocity can be measured by using Ultrasonic Doppler Method (UDM) [1, 2]. For void fraction, there are many studies related to measurement of this parameter by ultrasonic technique. Utomo et al. [3, 4] employed ultrasonic signal and neural network to obtain cross-sectional void fraction, mean bubble diameter and solid hold-up in both an air-water bubble column and a slurry bubble column. The energy attenuation and the transmission time difference of ultrasound from a transmitter to a receiver are measured at the same position with cross-sectional void fraction measured by a non-intrusive optical method. The neural network is employed to develop relation between the parameters of the ultrasonic signal and the hydraulic parameters. The accuracy of this measurement technique is good compared with experimental data and other research work. Supardan et al. [5, 6] also employed ultrasonic signal and neural network to obtain cross-sectional void fraction and volumetric mass transfer coefficient in both non-reacting and reacting bubble columns. The energy attenuation and the transmission time difference of ultrasound from a transmitter to a receiver are measured at the same position with cross-sectional void fraction and volumetric mass transfer coefficient measured by a non-intrusive optical method and a dissolved oxygen probe, respectively. The neural network is employed to develop relation between the parameters of the ultrasonic signal and the hydraulic parameters. The accuracy of this measurement technique is good compared with experimental data and other research work. However, this measuring technique can obtain only cross-sectional void fraction. Warsito et al. [7] developed Ultrasonic Computed Tomography (UCT) by using three pairs of ultrasonic probes and tomographic reconstruction technique for obtaining local void fraction in a slurry bubble column. The energy attenuation and the time difference of the transmission signal are measured and reconstructed to be local void fraction. The accuracy of this method is compared by the result by other work. This technique can obtain local void fraction so some behaviors of asymmetrical bubbly flow along column length can be shown in this study. However, this method might be too complicated and expensive for symmetric bubbly flow.

From this view point, the main objective of my study is to develop local void fraction measurement in symmetric bubbly flow by reflected ultrasonic technique intensity with a transducer probe. However, this paper presents only the first step of a whole work. In this paper, patterns of instantaneous reflected ultrasonic intensity profiles along an ultrasonic beam of various bubbly flow conditions are investigated. Local void fraction profiles are measured by Wire Mesh Tomography (WMT) at same position with an ultrasonic probe.

2. Experimental Setup

2.1 Experimental apparatus

The experimental apparatus is an air-water vertical acrylic pipe with inside diameter of 50 mm as illustrated in Figure 1. Total height of the apparatus is about 7 m (140 L/D_H). Water is supplied from storage tank (No. 7). Water is injected through the bubble generation (No. 4). Water low rate is controlled using a control valve (No. 8). The volumetric water flow rate is measured by an orifice flow meter (No. 6). The bubble generator is illustrated in Figure2. This bubble generator is composed by liquid main flow, defined using U_L, liquid sub flow, defined using U_{sub}, and gas flow, defined using U_G. Inside the bubble generator, air is supplied from the air chamber through holes and injected into the pipe through a ring gap of 1 mm. The bubble size is controlled by gas, liquid main and sub flow and number and size of holes inside the bubble generator. The 4 holes of 0.4 mm diameter were drilled in the air-chamber wall at the same distance and same height in order to generate the equal size of bubbles. The four Mass-Flow controllers (STEC, SEC-E40- 200SCCM) were installed to control the gas flow-rate at each hole. Each Mass-Flow controller is connected to each holes the bubble generator to control the gas flow rate precisely and uniformly to generate symmetrical bubbly flow. The volumetric water flow rate of sub-flow is measured by an orifice flow meter. The volumetric air flow rate is measured upstream of the air injection needles by a laminar flow meter (No. 16) with an accuracy of ± 1.5 %. Flow conditions of this work are investigated at L/D = 43. The utilized flow conditions of this experiment are summarized in the Table 1.

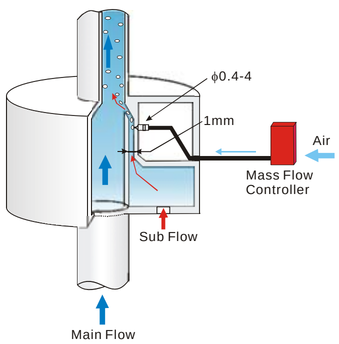

Figure 2 Bubble generator

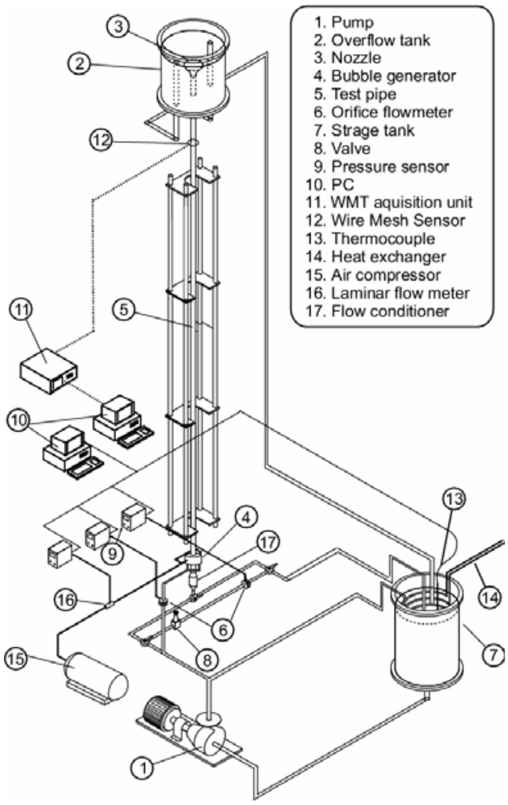

Figure 1 Experimental setup

Table 1 Experimental condition

Condition	Water flow condition Re base on pipe 50 mm		U_G (m/s)
1	4000	4000	0.00103
2			0.00206
3			0.00309
4	5000	3000	0.00103
5			0.00206
6			0.00309
7	6000	2000	0.00103
8			0.00206
9			0.00309
10	7000	1000	0.00103
11			0.00206
12			0.00309
13	8000	0	0.00103
14			0.00206
15			0.00309

2.2 Ultrasonic system

An ultrasonic transducer was set up at 45 degrees. The basic frequency and the beam diameter are 2MHz and 10 mm, respectively. A pulse ultrasound is transmitted from the transducer connected to an ultrasonic Pulser /Receiver (DPR300: JSR Ultrasonic Inc.). The same transducer detects the reflected US from a boundary of water and bubble, and then the signal amplified by the receiver is recorded using a digital oscilloscope (C574L: LeCroy Inc.). The basic specifications of ultrasonic measuring system are listed in Table 2- 5.

Table 2 Specification of ultrasound

Basic frequency	2 MHz
Beam diameter	10 mm
Incident angle	45 degrees

Table 3 Specifications of an ultrasonic pulser

Pulse type	Negative spike
Initial transition (Fall time)	< 5 ns
Input voltage : V_{input}	150 V
Pulse energy	3.49 μ J
Damping impedance	331 Ω
PRF : F_{PRF}	400 Hz

Table 4 Specifications of an ultrasonic receiver

Gain : G_R	38 dB
Bandwidth	0.001 to 35 MHz
High pass filter	1.0 MHz
Low pass filter	7.5 MHz

Table 5 Specifications of a digital oscilloscope

Sample rate	25 MS/sec
Resolution of ADC	8 bit
Memory	4 MB
Clock accuracy	$\leq$10 ppm
DC accuracy	$\pm$ 1%

An intensity of a reflected ultrasonic signal depends on specifications of an ultrasonic system, which consist of an ultrasonic pluser/receiver, a transducer and a digital oscilloscope. Therefore, in this study, reflected ultrasonic signal is defined as following

$$E = 10\log\frac{P_{output}}{P_{input}} = 20\log\frac{V_{output}}{V_{input}} - G_R \qquad (1)$$

When *P* mean input and output power, V_{input} and V_{output} are peak to peak voltage transmitted by a pulser and obtained by a digital oscilloscope, respectively, and G_R is gain using a receiver.

2.3 Wire mesh Tomography (WMT)

The circular wire mesh sensor is illustrated in Figure 3 was designed to cover an entire circular cross-section of 50 mm inside diameter. Three electrode wire layers of square grid are placed through the pipe wall separated from each other by 2 mm. The middle plane is a transmitter plane while the upper and lower planes are receiver planes. Local instantaneous electrical conductivity is directly measured between each pairs of crossing wire. Each wire layer consists of 16x16 wires corresponding to the spatial resolution of 2.94x2.94 mm^2 with the wire diameter of 0.125 mm.

Data acquisition unit is a commercial product from Teletronic Rossendorf GmbH. It has a maximum overall sampling frequency of 10 kHz. It has a maximum capacity of 170,000 frames. The entire signal acquisition procedure is controlled by a Digital Signal Processor (DSP). The obtained data is stored in the buffer memory of the acquisition unit and transferred to a personal computer. Information on the 10 kHz acquisition unit is described in detail by Prasser et al. [9].

The principle of WMT is based on local conductivity measurement in a gap between each electrode pair crossing. The sensor delivers a sequence of two-dimension distributions of local instantaneous conductivity, measured in each mesh formed by two crossing wires. Local instantaneous void fractions are calculated assuming linear dependence between void fraction and conductivity. Thus, the measured conductivity values are related to calibration values obtained for plain liquid in the measuring plane. The result is a three-dimensional data array $\alpha(x, y, t)$ where t is the instantaneous void fraction distribution in time sequence and x, y are the local measurement positions in the cross section. The local time dependent void fraction can be obtained directly from the linear relation with the measured electrical conductivity in the following

$$\alpha(x,y,t) = \frac{V(x,y,t) - V(x,y)^W}{V(x,y)^A - V(x,y)^W} \qquad (2)$$

Where $V(x,y)^A$ and $V(x,y)^W$ are the voltage corresponding to plain air (α =100%) and plain water (α = 0%) respectively. Local time- averaged void fraction is directly averaged from local time-dependent void fractions for 10 seconds.

For accuracy of WMT on void fraction measurement, there are many studied trying to clarify the accuracy of WMT. Prasser et al. [8], compared cross-sectional void fraction with other measurement methods, a non-intrusive optical method and Gamma-densitometer. The deviation is very good. Furthermore, Prasser et at. [9] also compared local void fraction measured by WMT with the one measured by ultra-fast X-ray tomography in an air-water system. The agreement of local void fraction measurement between these two measurement methods is very good. The deviation is within 10%. Therefore, WMT can be used for reference of local void fraction measurement method.

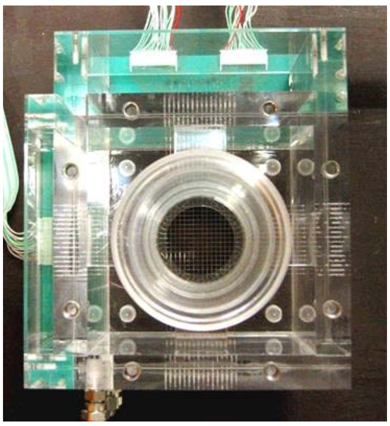

Figure 3 Wire Mesh Sensor

4. Result and Discussion

4.1 Spatio-temporal Distribution

Spatio-temporal distributions of many types of bubbly flow are illustrated in Figure 4(a)-(c), respectively, to estimate the alteration of reflected ultrasonic signal from moment to moment. The signals passing the noise level intensity are plotted in these Figures. The horizontal axis means the time up to 3.72 seconds and the vertical axis means the distance from the center of a pipe to the wall of the pipe that is near the transducer. The spatio-temporal reflected US of Wall-peak bubbly flow, Re_{main}=4000, Re_{sub}=4000, J_G = 0.00206 m/s, is shown in Figure 4(a). Most of the signal appears at the near region of the transducer. The spatio-temporal reflected US of flat profile bubbly flow, Re_{main}=7000, Re_{sub}=1000, J_G = 0.00206 m/s, is shown in Figure 4(b). The signal appears uniformly in a cross-sectional of a pipe. The spatio-temporal reflected US of Wall-peak bubbly flow, Re_{main}=8000, Re_{sub}=0, J_G = 0.00206 m/s, is shown in Figure 4(c). Most of the signal appears at the center of a pipe. The radial profile of averaged and standard deviation of reflected intensity is calculated from the spatio-temporal distribution. The averaged and standard deviation of reflected ultrasonic intensity of many kind of bubbly flow is illustrated in next section.

4.2 Experimental data of local void fraction by WMT and Characteristic of reflected ultrasonic intensity in air-water bubbly flow

Reflected ultrasonic intensity along an ultrasonic beam and local void fraction distribution from WMT of Re main = 4000 and Re sub = 4000, Re main = 6000 and Re sub = 2000, Re main = 7000 and Re sub = 1000,Re main = 8000 and Re sub = 0 are shown in Figure 5(a-c), Figure 6 (a-c), Figure 7(a-c) and Figure 8 (a-c), respectively. From Figure 5-6 (a and b), the average and standard deviation of reflected ultrasonic intensity in wall-peak void fraction profile are displayed. This condition is recognized to be a wall peak void fraction profile condition by WMT, shown in Figure 5-6 (c). For the wall-peak void fraction profile, there are higher averaged and stand deviation values at near wall area because of the high probability of reflected signal near wall area. The average and standard deviation of statistical distributions of reflected ultrasonic intensity in Re_{main} of 7000 and Re_{sub} of 1000 conditions are displayed in Figure 7 (a and b). This condition is recognized to be flat profile void fraction profile condition by WMT, shown in Figure 7(c). For the flat profile void fraction profile, there are averaged and stand deviation values uniformly in the whole of the cross – section of a pipe. The average and standard deviation of statistical distributions of reflected ultrasonic intensity in Re_{main} of 8000 and Re_{sub} of 0 conditions are displayed in Figure 8 (a and b). This condition is recognized to be a core peak void fraction profile condition by WMT, shown in Figure 8(c). For the core-peak void fraction profile, there are higher averaged and stand deviation values at center of pipe area because of the high probability of reflected signal at center of pipe area. The averaged and standard deviation of reflected ultrasonic intensity of wall, flat profile and core peak profile are different pattern. However, for each type of void fraction profile, the averaged and standard deviations of reflected ultrasonic intensity patterns are same. The pattern of reflected ultrasonic of J_G of 0.00109 m/s J_G of 0.00219 m/s and J_G of 0.00328 m/s are same in each liquid condition, as shown in Figure 5- 8 (a and b). This experimental data will be database for developing neural network. The neural network could be employed to develop relation between parameters of reflected ultrasonic intensity and local void fraction in the future work. The database will be separated in two categories, training database and testing database. The training data is employed for developing the neural network. The testing data is employed to test the developed neural network.

5. Conclusion

This study applies ultrasonic signal and measures strength of reflected intensity from bubbles in an air-water system. The experimental apparatus using in this study is a circular acrylic pipe with an inner diameter of 50 mm. A Wire Mesh Tomography (WMT) method is also applied to measure local void fraction at same position with an ultrasonic probe. Spatio-temporal distributions of reflected ultrasonic intensity along an ultrasonic beam in various bubbly flow conditions are investigated and reported. The spatio-temporal distribution of each local void fraction profile is different. The reflected ultrasonic intensity appears more often at near wall position in wall-peak bubbly flow while the reflected ultrasonic intensity appears more often at the center of a pipe in core-peak bubbly flow. For flat profile bubbly flow, the reflected ultrasonic intensity appears uniformly in the whole cross-section of a pipe. The averaged and standard deviation of reflected ultrasonic intensity and local void fraction in wall-peak, core-peak and flat void fraction bubbly flow are also shown and discussed. These three parameters will be employed for database in development of local void fraction measurement by using reflected ultrasonic intensity in the future work.

Acknowledgments

The authors wish to acknowledge the valuable contributions and financial support of Dr. Hiroshige Kikura and Prof.Masanori Aritomi, Research Laboratory for Nuclear Reactor, Tokyo Institute of Technology, Japan

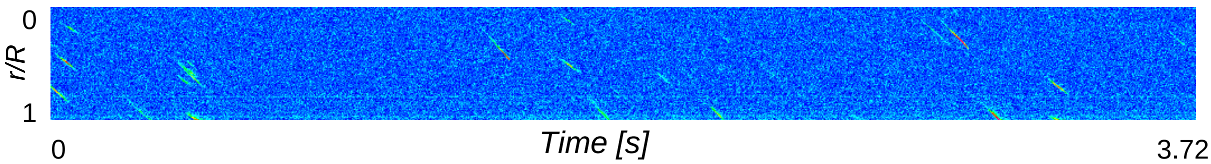

Figure 4(a). Spatio-temporal reflected US of Wall-peak bubbly flow(Re $_{main}$=4000, Re $_{sub}$=4000 , JG = 0.00206 m/s)

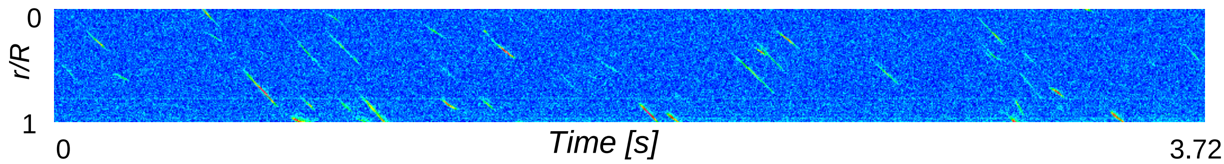

Figure 4(b) Spatio-temporal reflected US of Flat profile bubbly flow(Re $_{main}$=7000, Re $_{sub}$=1000 , JG = 0.00206 m/s)

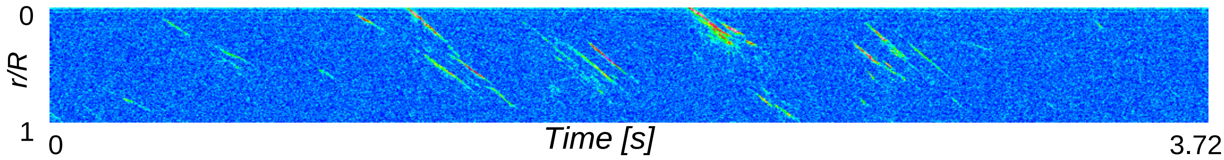

Figure 4 (C) Spatio-temporal reflected US of Core-peak bubbly flow(Re $_{main}$=8000, Re $_{sub}$=0000 , JG = 0.00206 m/s)

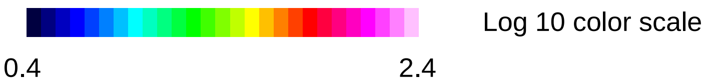

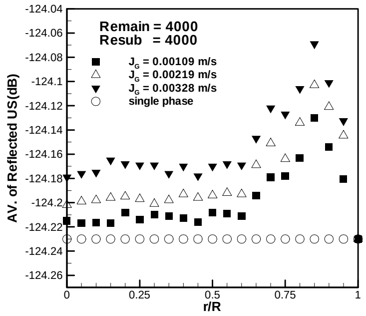

Figure 5(a) Average of reflected US intensity of Re $_{main}$=4000, Re $_{sub}$=4000

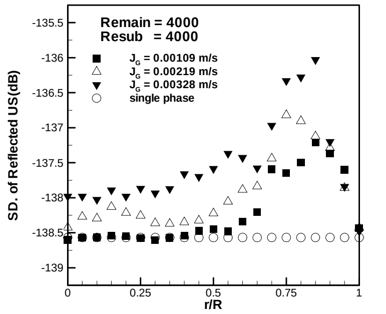

Figure 5(b) Standard deviation of reflected US intensity of Re $_{main}$=4000, Re $_{sub}$=4000

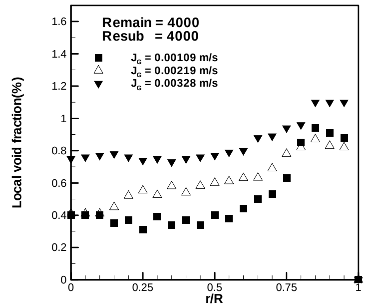

Figure 5(c) Local void fraction of Re$_{main}$=4000, Re $_{sub}$=4000

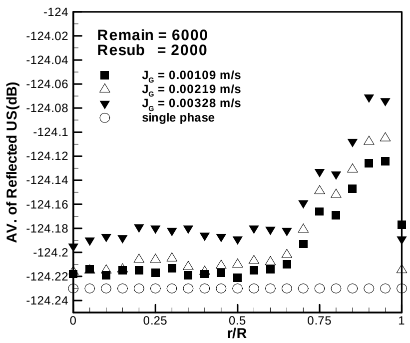

Figure 6(a) Average of reflected US intensity of Re $_{main}$=6000, Re $_{sub}$=2000

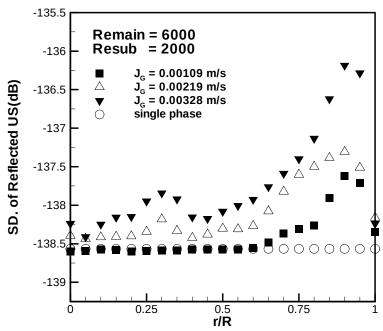

Figure 6(b) Standard deviation of reflected US intensity of Re $_{main}$=6000, Re $_{sub}$= 2000

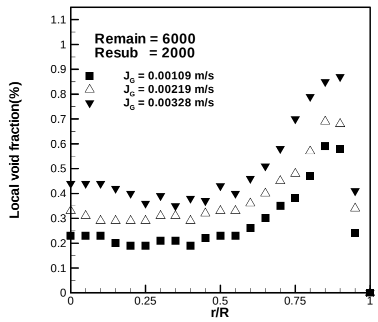

Figure 6(c) Local void fraction of Re $_{main}$=6000, Re $_{sub}$= 2000

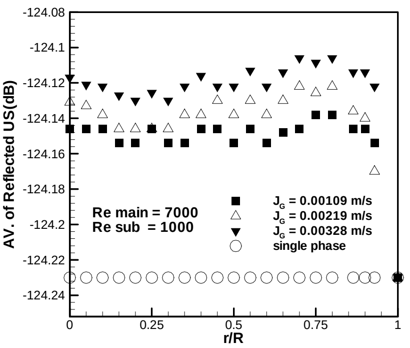

Figure 7(a) Average of reflected US intensity of Re $_{main}$=7000, Re $_{sub}$=1000

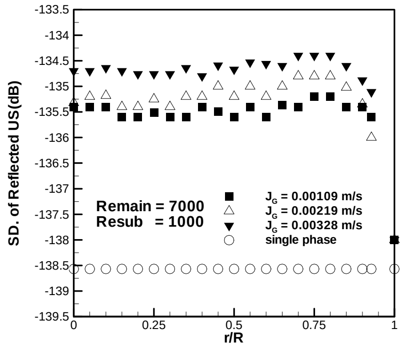

Figure 7(b) Standard deviation of reflected US intensity of Re $_{main}$=7000, Re $_{sub}$=1000

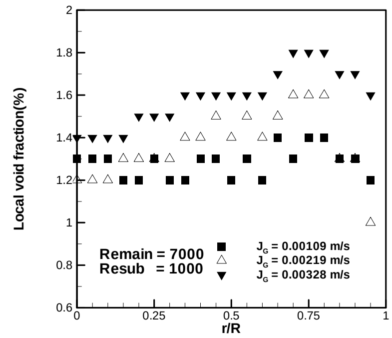

Figure 7(c) Local void fraction of Re $_{main}$=7000, Re $_{sub}$=1000

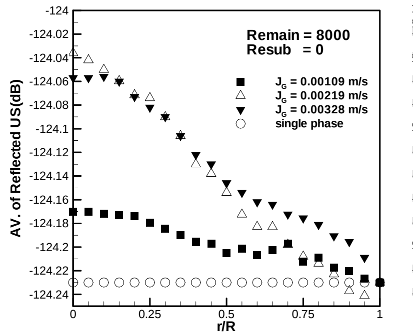

Figure 8(a) Average of reflected US intensity of Re $_{main}$=8000, Re $_{sub}$= 0000

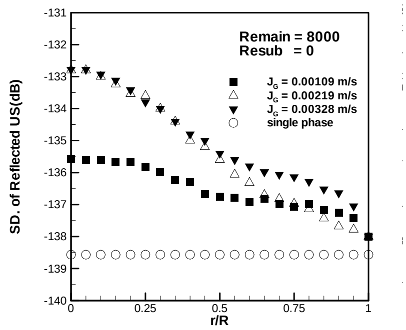

Figure 8(b) Standard deviation of reflected US intensity of Re $_{main}$=8000, Re $_{sub}$= 0000

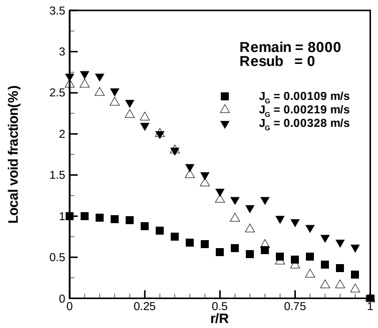

Figure 8(c) Local void fraction of Re $_{main}$=8000, Re $_{sub}$= 0000

References

[1] S.Wada, H.Kikura,M.Aritomi, M.Mori, Y.Takada, “ Development of pulse ultrasonic Doppler method for flow rate measurement in power plant on multilines flow rate measurement on metal pipe” ,Journal of Nuclear science and technology, Vol.41,No.3,pp. 339-346, March 2004

[3] Marsudi B. Utomo, T. Sakai, S. Uchida and A. Maezawa, “Simultaneous Measurement of Mean Bubble Diameter and Local Gas Holdup Using Ultrasonic Method with Neural Network”, Chem.Eng.Technology, Vol. 24, No.5,pp. 493-500,2001

[4] Marsudi B. Utomo, T. Sakai and S. Uchida, “Use of Neural Network-Ultrasonic Technique for Measuring Gas and Solid Hold-ups in a Slurry Bubble Column”, Chem.Eng.Technology, Vol. 25, No.3,pp. 293-299,2002

[5] M.D. Supardan, A. Maezawa and S. Uchida, “Determination of Local Gas Holdup and Volumetric Mass Transfer Coefficient in a Bubble Column by Means of an Ultrasonic Method and Neural Network”,Chem.Eng.Technology, Vol. 26, No.10, pp. 1080-1083,2003

[6] M.D. Supardan, Y. Masada, Y. Maezawa and S. Uchida, “Local Gas Holdup and Mass Transfer in a Bubble Column Using an Ultrasonic Technique and Neural Network”, Journal of Chemical Engineering of Japan, Vol. 27, No.8, pp. 927-932,2004

[7] Warsito, M. Ohkawa, N. Kawata, S. Uchida, “Cross-sectional distributions of gas and solid holdups in slurry bubble column investigated by ultrasonic computed tomography”, Chemical Engineering Science, Vol. 54, pp. 4711-4728, 1999

[8] H.M. Prasser, A. Boltger, J.Zccchau, A new electrode-mesh tomography for gas-liquid flow, Flow measurement and Instrumentation, vol.9, pp. 111-119, 1998

[9] H.M. Prasser, M. Misawa and I. Tiseanu, Comparison between wire-mesh sensor and ultra-fast X-ray tomography for an air-water flow in a vertical pipe, Flow measurement and Instrumentation, vol.16, pp. 73-83, 2005